Wiley
Advances in Pharmacological and Pharmaceutical Sciences
Volume 2026, Article ID 1686964, 15 pages
https://doi.org/10.1155/adpp/1686964

WILEY

Research Article

Alternanthera philoxeroides (Mart.) Griseb Mitigates Age-Related Depression in Mice Through Regulation of Oxidative Stress and Neurogenic Mechanisms

Possatorn Aon-im,[1] **Orawan Monthakantirat**,[2] **Yaowared Chulikhit**,[2] **Supawadee Daodee**,[2] **Chantana Boonyarat**,[2] **Anake Kijjoa**,[3] **and Charinya Khamphukdee**[1]

[1]*Division of Pharmacognosy and Toxicology, Faculty of Pharmaceutical Sciences, Khon Kaen University, Khon Kaen 40002, Thailand*
[2]*Division of Pharmaceutical Chemistry, Faculty of Pharmaceutical Sciences, Khon Kaen University, Khon Kaen 40002, Thailand*
[3]*School of Medicine and Biomedical Sciences Abel Salazar (ICBAS) and CIIMAR, Universidade do Porto, Rua de Jorge Viterbo Ferreira 228, Porto 4050-313, Portugal*

Correspondence should be addressed to Charinya Khamphukdee; charkh@kku.ac.th

Received 21 May 2025; Revised 27 August 2025; Accepted 16 December 2025

Academic Editor: Anjali Chauhan

Copyright © 2026 Possatorn Aon-im et al. Advances in Pharmacological and Pharmaceutical Sciences published by John Wiley & Sons Ltd. This is an open access article under the terms of the Creative Commons Attribution License, which permits use, distribution and reproduction in any medium, provided the original work is properly cited.

Depression adversely impacts daily life, with age-related neurodegeneration being a significant contributing factor. Neurodegenerative alterations, often accelerated by oxidative stress, underlie depressive progression in advanced age. Our previous research has reported that *Alternanthera philoxeroides* (Mart.) Griseb (AP) exhibits promising antioxidant properties for counteracting age-related dementia. However, other mechanisms, such as those related to aging-induced depression, have not been investigated. The present study investigated the therapeutic potential of AP against D-galactose (D-gal)-induced geriatric depression in male mice, with a specific emphasis on its antioxidative properties and neurogenesis-mediated mechanisms of action. AP extract showed radical scavenging activity by transferring hydrogen atoms and single electrons. Moreover, AP treatment significantly restored the endogenous defensive system and neuronal regeneration, prevented lipid peroxidation in mood-regulating brain regions, and reduced serum corticosterone levels, alleviating depressive-like behaviors. Nuclear magnetic resonance (NMR)–based metabolomic pathway analysis revealed that neurotransmitter synthesis, energy production, and protein synthesis were the pathways modulated by AP. Thus, AP extract demonstrated neuroprotective and antidepressive effects in aging-induced depression, offering a promising source for the treatment of depression in elderly patients. Further research is required to establish its role in treating aging-related neurodegenerative diseases.

Keywords: aging; *alternanthera philoxeroides* (AP); D-galactose (G-gal); depression; metabolomics; oxidative stress

1. Introduction

Aging-induced depression, or geriatric depression, is characterized by mood disturbances, cognitive impairment, and diminished daily functioning. In aging brains, reactive oxygen species (ROS) such as hydroxyl radical (•OH) and hydrogen peroxide (H_2O_2) accumulate, causing oxidative damage to neurons and lipid peroxidation within brain tissues [1]. Additionally, increased levels of corticosterone, a marker of chronic stress caused by the loss of hypothalamic–pituitary–adrenal (HPA) axis negative feedback, in the aged brain further contribute to neurodegeneration and therefore depression [2].

Pharmacological interventions for depression aim to enhance mood by modulating neurotransmitter levels and protecting against neurodegeneration. Antidepressive

agents increase the availability of serotonin, norepinephrine, and dopamine in the brain. Nevertheless, the long-term use of conventional antidepressants can cause side effects, and their efficacy in the treatment of age-related depression remains inconsistent [3]. Thus, exploring naturally occurring compounds with antidepressive properties, particularly those with additional neuroprotective effects, can be a good avenue to discover natural antidepressant drugs.

In Thai ethnomedicine, the whole plant of *Alternanthera philoxeroides* (Mart.) Griseb (AP) (family Amaranthaceae) is applied as a therapeutic agent for antipyretic, venom neutralization, blood improvement, and galactagogue effects, and management of postpartum depressive disorders [4]. AP exhibits various neuroprotective, i.e., antioxidant, anti-inflammatory, and antidementia effects [5]. AP was found to possess antidepressive effects in ovariectomized (OVX) mice, which was attributed to its estrogenic activity. The phytochemical constituents, including Alternanthin, Alternanthin B, Chrysoeriol 7-O-rhamnoside, Demethyltorosaflavone D, and Torosaflavone E, were found to display monoamine oxidase (MAO) inhibitory activities [6]. However, other mechanisms, such as those related to aging-induced depression, have not been investigated. Subcutaneous injection of D-galactose (D-gal) has been used as a model for aging-induced depression. Chronic administration of D-gal led to an accumulation of advanced glycation end products (AGEs), stimulating excessive free radical production. Consequently, the endogenous antioxidant system was unable to overcome free radical damage, causing neurodegeneration [7]. This phenomenon led to neuronal dysfunction, which results in anxiety, depression, and memory impairment [8].

The current study aimed to investigate the antidepressive effects of AP against D-gal–induced depression in ICR mice by elucidating the role of AP in counteracting aging-associated depression. This study can lead to the development of effective natural therapeutics that target both neurodegenerative and mood disorders in aging populations.

2. Materials and Methods

2.1. Plant Material Extraction Procedure. The whole plant of AP was bought from Dai Sai Market as a vegetable, Dai Sai District, Loei province, Thailand, in August 2022 prior to deposition at the herbarium of the Faculty of Pharmaceutical Sciences of Khon Kaen University, Thailand, with the voucher specimen (KKPH010102986). Dried powder of AP (1 kg) was the Soxhlet extract with EtOH (3 × 10 L) at 50°C for 2 h. The solvent was then evaporated using a rotary evaporator at 50°C, and the remaining residue was further dried by freeze-drying. The freeze-dried powder of this extract was kept at −20°C throughout the experiment. Phytochemical composition of AP was identified and qualified using high-performance liquid chromatography (HPLC), with the validated analytical method previously described by Aon-im et al. The Hypersil ODS Columns (C18, 250 × 4.6 mm, 5 μm, particle size) were used in the reversed-phase HPLC system. The injection volume was 20 μL, and the column compartment was maintained at 25°C. The detection was observed at 254, 275, 330, and 370 nm. Acetonitrile (Solvent A) and 10% 2-propanol in 1% aqueous formic acid (Solvent B) constituted the gradient solvent system at a controlled flow rate of 1 mL/min, following the gradient elution reported in the previous study [9]. Isolated compounds were obtained from a partition fraction of EtOAc, which was applied to a silica gel column and eluted with petrol-$CHCl_3$ and $CHCl_3$–Me_2CO, respectively. Subfractions were subsequently applied to a Sephadex LH-20 column and eluted with MeOH and $CHCl_3$. Crystallization, precipitation, and preparative TLC techniques were employed to isolate pure compounds. This methodology was previously reported by Khamphukdee et al. [6].

2.2. Radical Scavenging Activity

2.2.1. Hydrogen Peroxide Scavenging Assay. A mixture of $(NH_4)_2$ $Fe(SO_4)_2{\cdot}6\,H_2O$ (Sigma-Aldrich, MO, USA) and H_2O_2 (Sigma-Aldrich, MO, USA) was incubated for 5 min with light protection before adding 1,10-orthophenanthroline (Sigma-Aldrich, MO, USA) and incubated for 10 min (25°C). Scavenging activity was calculated from the percentage ratio of absorbance of the test compound and the control, at 510 nm. The results were reported as a half-maximal inhibitory concentration (IC_{50}) [10].

2.2.2. Hydroxyl Radical Scavenging Assay. Reagents were purchased from Sigma-Aldrich, MO, USA. Hydroxyl radical scavenging assay was performed according to the method described by Roghini and Vijayalakshmi [11]. Preparation of the following reagents was carried out: The initial solution contained deoxyribose (10 mM), disodium EDTA (1 mM), aqueous extraction (60 μL), ferric chloride (10 mM), and phosphate buffer (50 mM). Thereafter, one mM ascorbic acid along with 10 mM hydrogen peroxide with 30 μL of each was added. The mixture was incubated at 37 °C for 1 h. Then, 0.5% thiobarbituric acid and 10% trichloroacetic acid with 360 μL of each were further added with subsequent incubation at 100 °C for 15 min. A 96-well microplate reader (Perkin Elmer Inc., Waltham, MA, USA) was used for absorption spectroscopy at 532 nm. Percent inhibition was further calculated for IC_{50}

2.2.3. Assay for DPPH Radical Scavenging. 2,2-Diphenyl-1-picrylhydrazyl (DPPH) (Sigma-Aldrich, MO, USA) was freshly prepared and protected from light after mixing with samples. Absorbance at 515 nm was measured and reported as the IC_{50} of scavenging activity [12].

2.2.4. Assay for Ferric Reducing Antioxidant Power (FRAP). The assay procedure was used with modifications from Skroza et al. Freshly prepared FRAP reagent (Sigma-Aldrich, MO, USA) was incubated with either test samples or Trolox (Sigma-Aldrich, MO, USA) for 5 min at 37°C. After measuring absorbance at 593 nm, the amount of Trolox

equivalent per 1 g of compound was determined as the antioxidant capacity [13].

2.3. Animals. Fifty male ICR mice, aged 5 weeks and weighing 20–30 g, were acquired from the Northeast Laboratory Animal Center, Khon Kaen, Thailand (License No. B2559/00015) and maintained in the animal room of the Faculty of Pharmaceutical Sciences, Khon Kaen University, Thailand. Humidity and temperature in the housing were controlled, with a 12-h light-dark cycle. After 1 week of acclimatization (5 mice/cage), the animal study protocol was carried out for 8 weeks by the oral administration of AP, followed by a subcutaneous injection of D-gal 150 mg/kg/day, 30 min after AP administration to accelerate aging. Behavioral studies were undertaken from the sixth week to the end. After behavioral test in each day, mice were housed in a cozy and quiet area with adequate food and water for recovery. Animals showing severe, unmanageable discomfort or pain were either removed from the study or humanely euthanized with an intraperitoneal injection of thiopental sodium at 80 mg/kg) according to ethical protocols to reduce suffering. The animal procedures in this investigation were performed in strict compliance with the Guiding Principles for the Care and Use of Animals (NIH Publications No. 80–23, 1996 revision) and were approved by the Institutional Animal Care and Use Committee at Khon Kaen University, Thailand (Record: IACUC-KKU-77/65; Reference: 660201.2.11/512(82)). The authors confirm that the study was conducted in compliance with the ARRIVE guideline (https://arriveguidelines.org/).

2.4. Experimental Interventions. Following one week of acclimatization, different interventions were conducted to five randomly allocated experimental groups ($n = 10$ per group), including corn oil p.o. (healthy control group), D-gal 150 mg/kg/day s.c. + corn oil p.o. (vehicle or negative control group), D-gal 150 mg/kg/day s.c. + Vitamin E 100 mg/kg/day p.o. (Vit. E or positive control group), D-gal 150 mg/kg/day s.c. + AP 250 mg/kg/day p.o. (AP250 group), and D-gal 150 mg/kg/day s.c. + AP 500 mg/kg/day p.o. (AP500 group) for eight consecutive weeks. D-gal was subcutaneously injected 30 min after oral administration of Vitamin E or AP. Figure 1 exhibits the details of this experimental design.

All behavioral testing was performed in the morning to control for circadian variability: All assays for each experimental group commenced with the first mouse at 07:00 h. The testing sequence for each animal was (1) FST preswim (15 min) on Day 57, (2) FST test (5 min) on Day 58 (first mouse 07:00 h), (3) TST on Day 59 (6 min per mouse; first mouse 07:00 h), followed by a full rest day (Day 60), and (4) locomotor assessment by the Y-maze test on Day 61 (8 min per mouse; first mouse 07:00 h). To accommodate equipment limitations, the 50 animals were divided into two equal cohorts of 25 mice each, and testing was simultaneously carried out in the mornings. Within each cohort, the order of mice was randomized, and animals from different treatment groups were distributed evenly across early and late testing times to reduce time-of-day bias. All handlers were trained in consistent handling, timing, and scoring procedures, and their agreement on scoring was checked before data collection. Mice were habituated to the testing room for approximately 30 min before the first daily assay. Between animals, the apparatus was cleaned, and mice were briefly dried after swim sessions to avoid hypothermia. This schedule ensured more than 24 h between preswim and FST, more than 24 h between FST and TST, and a full day of recovery before Y-maze testing, minimizing carryover and time-of-day confounds.

2.5. Test for Depressive-Like Behaviors

2.5.1. Tail Suspension Test (TST). Mice were attached by adhesive tape to their tails, 30 cm above the ground and suspended upside down. Hopeless behavior was evaluated by recording the immobility time (4 min) after the habituation period (2 min). Dark conditions were maintained during TST to avoid interference from environmental factors [14].

2.5.2. Forced Swimming Test (FST). Mice were placed in a water-filled cylindrical container (12 cm width x 25 cm height) from which escape was impossible, and the water was maintained at 25°C and reached a depth of 10 cm. Twenty-four hours before test sessions, mice were forced to swim freely for 15 min, and they were further placed in a constant stressful condition. Immobility time was noted during the test sessions for 5 min [15].

2.5.3. Locomotor Activity (LA). To prove that the LA or movement was not affected as a result of each intervention, the Y-maze test with arm entries enumerated across a standardized 5-min testing session was performed [16].

2.6. Blood and Tissue Collection. The mice were sacrificed after anesthesia with an intraperitoneal injection of thiopental sodium (Jagsonpal Pharmaceuticals, Haryana, India) at 60 mg/kg. All animals were gently handled to reduce stress. The blood (1 mL) was collected by cardiac puncture technique between ZT4 and ZT6 (4–6 h after lights on, approximately 11:00–13:00 under a 12:12-h light–dark cycle) to minimize circadian variation, and then, the animals were perfused with 0.5% normal saline until the organs were clean prior to collecting the hippocampus and frontal cortex. The serum was separated from the blood by centrifugation at 3000 rpm at 21°C for 20 min and stored at −80°C [9].

2.7. Serum Corticosterone Determination. To determine serum corticosterone levels, a commercial corticosterone ELISA kit from ABclonal Technology was used following the manufacturer's instructions. Briefly, the serum (25 μL) was added into the 96-well microplates, followed immediately by 25 μL of biotinylated corticosterone per well. After gentle mixing and 2-h room temperature incubation, the wells were washed five times with 200 μL wash buffer. Then, 50 μL of streptavidin-peroxidase conjugate was added to each well and incubated for 30 min. Following another five washing cycles, 50 μL of chromogen substrate was added with a 20-

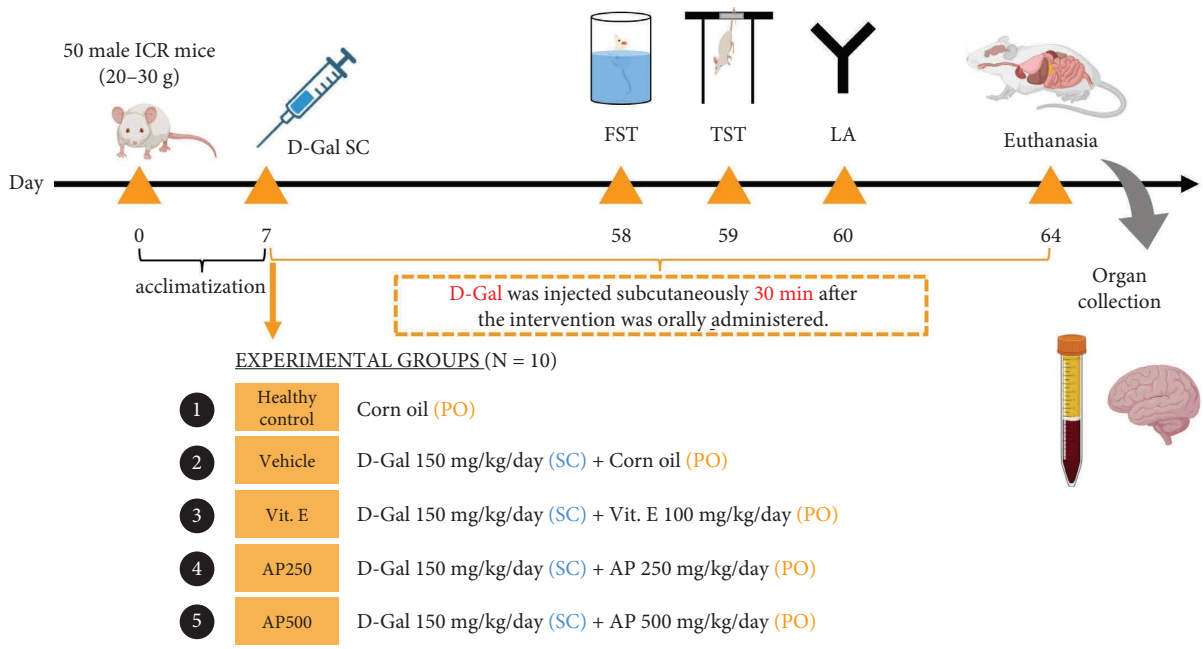


Figure 1: Schematic representation of the age-related depression model induced by D-gal in mice.

min incubation period. The reaction was terminated with 50 µL of stop solution, and absorbance readings were taken immediately at 450 nm [16].

2.8. Measurement of Lipid Peroxidation Activity. Oxidative stress in homogenized brain tissue was assessed via lipid peroxidation using the thiobarbituric acid reactive substance (TBARS) assay according to the protocol described by Maneenet et al. [15]. The protein content was determined using the Bradford dye reagent (Bio-Rad, Hercules, CA, USA) with bovine serum albumin (Sigma-Aldrich, MO, USA) as the protein standard. MDA (Sigma-Aldrich, MO, USA) levels were reported as nanomoles MDA per gram of protein.

2.9. Neurochemical Analysis via Quantitative Real-Time PCR. Neuropharmacological effects of AP on depression were examined using qPCR according to Chalermwongkul et al. [16]. ß-Actin was used as the reference gene, and target gene expressions were expressed in relative fold difference with the calculation by the $2^{-\Delta\Delta Ct}$ technique. PCR primers specific to ß-actin, Nrf2, Keap1, CREB, and BDNF genes were produced by Macrogen (Seoul, South Korea): (1)-ß-actin: 5′-AAC GGT CTC ACG TCA GTG TA-3′ (sense) and 5′-GTG ACA GCA TTG CTT CTG TG-3′ (antisense); (2)-Nrf2: 5′-ACA CGG TCC ACA GCT CAT C-3′ (sense) and 5′-TGC CTC CAA AGT ATG TCA ATC A-3′ (antisense); (3)-Keap1: 5′-TAC GAT GTG GAA ACA GAG ACG TGG A-3′ (sense) and 5′-ACA GGT ACA GTT CTG GTC AAT CT-3′ (antisense); (4)-CREB: 5′-TAC CCA GGG AGG AAT AC-3′ (sense) and 5′-GAG GCT GCT TGA ACA ACA AC-3′ (antisense); (5)-BDNF: 5′-GAC AAG GCA ACT TGG CCT AC-3′ (sense) and 5′-CCT GTC ACA CAC GCT CAG CTC-3′ (antisense).

2.10. Untargeted Nuclear Magnetic Resonance (NMR) Metabolomics Analysis. Serum metabolomic profiling was conducted by Khon Kaen University International Phenome Laboratory. The serum was centrifuged at 10,000 × *g* for 15 min at 4°C, after which, 300 µL of the supernatant was carefully extracted and transferred to a fresh tube, and mixed with an equal volume (300 µL) of a serum buffer (pH 7.4). Then, 550 µL of the mixture was transferred to the NMR tube, and the solution was reconstituted using 1 mL of serum buffer (pH 7.4) containing 0.075 M Na_2HPO_4, 2 mM NaN_3, and 0.08% TSP solution. A 400 MHz NMR spectrometer (Bruker Ascend™ 400, Bruker Biospin, Karlsruhe, Germany) equipped with a cryoprobe was used to obtain the ^1H NMR spectra of each sample. The samples were further examined by a 64-scan Carr–Purcell–Meiboom–Gill pulse sequence with the NMR tube (outside diameter of 5 mm) filled with 600 µL of sample. The KEGG database was used in MetaboAnalyst (https://www.metaboanalyst.ca accessed on March 22, 2025) to obtain the statistically significant pathways.

2.11. Statistical Analysis. Animal study: Randomization was carried out by assigning animals to groups using random number generation following the acclimatization period. Allocation concealment was maintained by ensuring that investigators responsible for administering treatments were not involved in behavioral scoring or biochemical analyses. Behavioral scoring was conducted by two independent observers who were blinded to group allocation, and interobserver consistency was established prior to data collection. Sample size determination was calculated by the "error degrees of freedom" (*E*) is calculated using formula **E = N–G**, where N is the total number of animals and *G* is the number of groups [17]. Statistical analyses included ANOVA with Tukey's test, PCA, and OPLS-DA from the

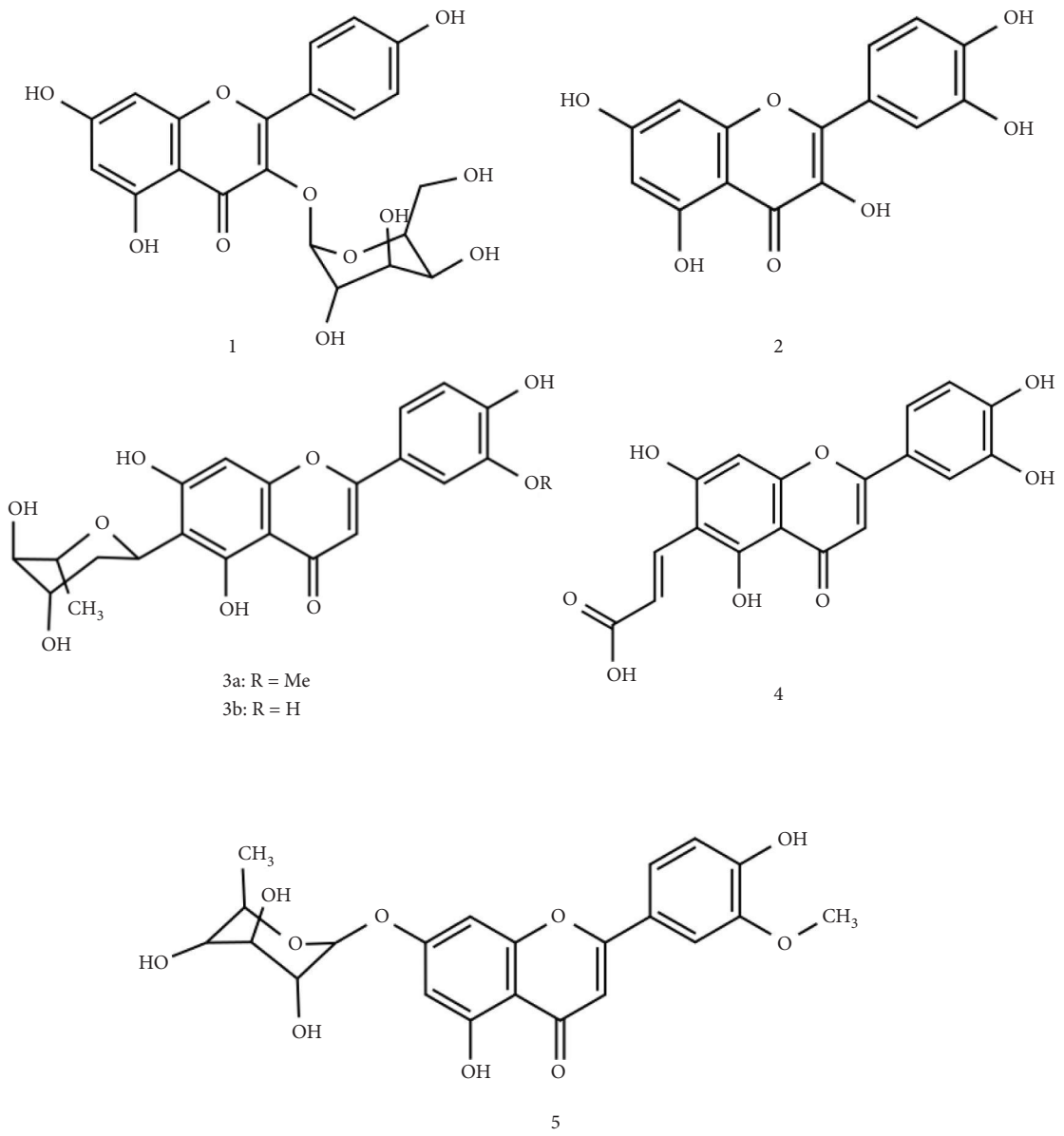


Figure 2: Chemical structures of kaempferol-O-glucoside (1), quercetin (2), alternanthin (3a), Alternanthin B (3b), Demethyltorosaflavone D (4), chrysoeriol-7-O-rhamnoside (5).

Python packages, and Bonferroni-corrected p values ($p < 0.05$) with VIP > 1.5 were considered significant [18].

3. Results

3.1. Phytochemical Profile of AP Extract. Six major active constituents, including kaempferol-O-glucoside (1), quercetin (2), alternanthin (3a), Alternanthin B (3b), demethyltorosaflavone D (4), and chrysoeriol-7-O-rhamnoside (5), were detected by the HPLC analysis of the AP extract (Figure 2) with the corresponding retention times of eluted peaks and standard compounds.

Peak separation in the HPLC chromatograms of all standards was acceptable (Supporting Information, Figure S1). The six compounds present in the AP extract were determined as 1.55 ± 0.09 mg/g extract for (1), 1.18 ± 0.18 mg/g extract for (2), 1.82 ± 0.03 mg/g extract for (3a), 1.39 ± 0.15 mg/g extract for (3b), 16.40 ± 1.22 mg/g extract for (4), and 2.34 ± 0.44 mg/g extract for (5).

3.2. AP Extract Exhibited Radical Scavenging Activity. The AP extract exhibited strong antioxidant activity, with IC_{50} values of 94.1 ± 0.6 and 386.8 ± 2.0 μg/mL for scavenging hydroxyl radicals and hydrogen peroxide, respectively. In addition, five isolated constituents, including alternanthin, Alternanthin B, Torosaflavone E, Demethyltorosaflavone D, and Chrysoeriol 7-O-rhamnoside, displayed potent free radical scavenging and reducing capacities as shown in Table 1. For example, the IC_{50} values against DPPH ranged from 34.4 ± 1.39 to 265.9 ± 18.51 μg/mL, while their FRAP activities ranged from 46.6 ± 4.96 to 1967.5 ± 66.69 μmol TEAC/g extract. The data represent the mean ± SD of triplicate.

Table 1: Antioxidative potential of AP extract and its isoflavone constituents.

Radical scavenging assay	IC_{50} for hydrogen peroxide (μg/mL)	IC_{50} for hydroxyl radical (μg/mL)	IC_{50} for DPPH (μg/mL)	FRAP value (μmol TEAC/g)
Trolox	619.7 ± 13.4	53.6 ± 0.1	11.4 ± 0.2	—
AP extract	386.8 ± 2.0	94.1 ± 0.6	—	—
1	—	—	265.9 ± 18.51	375.2 ± 23.87
2	—	—	48.6 ± 6.47	1967.5 ± 66.69
3	—	—	81.4 ± 1.53	88.1 ± 2.91
4	—	—	34.4 ± 1.39	327.0 ± 5.85
5	—	—	68.4 ± 1.95	46.6 ± 4.96

3.3. Depressive-Like Behaviors Were Ameliorated by AP Treatment. Evaluation of the antidepressive effects of the AP extract was associated with the mice's instinctive attempt to survive stressful conditions such as physical restraint and swimming. Thus, TST and FST were applied to investigate behavioral despair. The recorded immobility time directly correlated with the mice's hopelessness. Subcutaneous injection of D-gal (150 mg/kg/day) aggravated hopeless behaviors by the significant elevation of immobility time in both TST and FST (Figures 3(a), 3(b)). These deteriorated effects were alleviated by the oral administration of AP (500 mg/kg/day), which was similar to Vitamin E (100 mg/kg/day). Furthermore, the total count of entries from the Y-maze test indicated nonsignificant LA (Figure 3(c)). Consequently, the false-positive results of depressive-like behaviors from the administration of AP extract were not detected.

3.4. Serum Corticosterone Level Indicated That AP Prevented Stress Response. Serum corticosterone level was associated with activation of the HPA axis, which is related to stress responsiveness. The D-gal vehicle–treated group displayed a significant elevation of corticosterone level, compared to the healthy control. However, the level of stress hormone was significantly decreased when the AP extract (500 mg/kg/day) or Vitamin E (100 mg/kg/day) was orally administered. Thus, the oral administration of both AP extract and Vitamin E ameliorated the stress response (Figure 4).

3.5. Oral Administration of AP Prevented Brain Lipid Peroxidation. Lipid peroxidation resulted from D-gal -induced oxidative stress in the brain. Figure 5 shows the deteriorated effects of the hippocampus and frontal cortex due to significantly increased MDA levels in D-gal vehicle–treated mice. The aggravated effects were prevented by the oral administration of AP, which significantly reduced lipid peroxidation in both neural areas.

3.6. AP Extract Restored the Endogenous Antioxidative System Along With Neurogenesis. CREB-BDNF and Nrf2-Keap1 pathways were closely associated with neuronal regeneration and cellular defense systems, respectively. The activation of these pathways was likely to be decreased in the D-gal vehicle–treated mice; however, it can be restored by AP treatment (Figures 6(a), 6(b), 6(c), 6(d)).

3.7. AP Administration Modulated the Identified Pathways. A total of 23 metabolites were identified by ^{1}H NMR metabolomics analysis in serum samples (Supporting Information, Table S2). The metabolites detected in the NMR spectra (Figure 7) included citrate, isoleucine, creatine, leucine, choline, valine, carnitine, 3-hydroxybutyrate, glucose, saturated lipids, unsaturated lipids, lactate, fumarate, alanine, tyrosine, acetate, histidine, phenylalanine, uracil, histamine, succinate, formate, very low-density lipoprotein (VLDL), and three unidentified metabolites.

The metabolomic dataset was visualized using a PCA score plot, and the overall apparent metabolic shift due to the intervention is depicted. Each point represents a distinct experimental sample. Interestingly, the experimental groups exhibited unique grouping patterns, with the second component performing as a separator. Figure 8 shows a clear comparative analysis.

Moreover, the results obtained from OPLS-DA, with its strong explanatory power ($R^2Y = 85\%–99\%$) and predictive ability ($Q^2 = 60\%–90\%$), showed that different treatments were associated with distinct metabolic changes (Figures 9(a), 9(b), 9(c), 9(d), 9(e), 9(f), 9(g), 9(h)). A 1000 time permutation test was conducted to confirm the validity of these results. To establish a null distribution and assess the statistical significance of the detected metabolic alterations, the resampling technique involving a random arrangement of the group labels was applied. The findings highlighted the individuality of the observed physiological alterations by implying a different metabolic response to each intervention.

A two-way ANOVA with Bonferroni-adjusted p values was used to analyze metabolite differences among the various interventions, highlighting distinct metabolic alterations. Due to the clear separation observed between the D-gal and AP500 groups, alterations in metabolite levels were detected. Specifically, the AP500-treated group (500 mg/kg/day) exhibited significantly elevated levels of isoleucine, leucine, valine, alanine, citrate, fumarate, tyrosine, phenylalanine, and uracil. These findings were confirmed based on stringent criteria, including regression coefficients (ß) > 1, VIP score > 1.5, and Bonferroni-adjusted $p < 0.05$ to minimize false-positive results (Supporting Information, Table S2). The robustness of the OPLS-DA model was supported by permutation testing, and the reported p value of 0.00999 confirmed that the group separation was greater than would be expected by chance (Supporting Information, Figure S2).

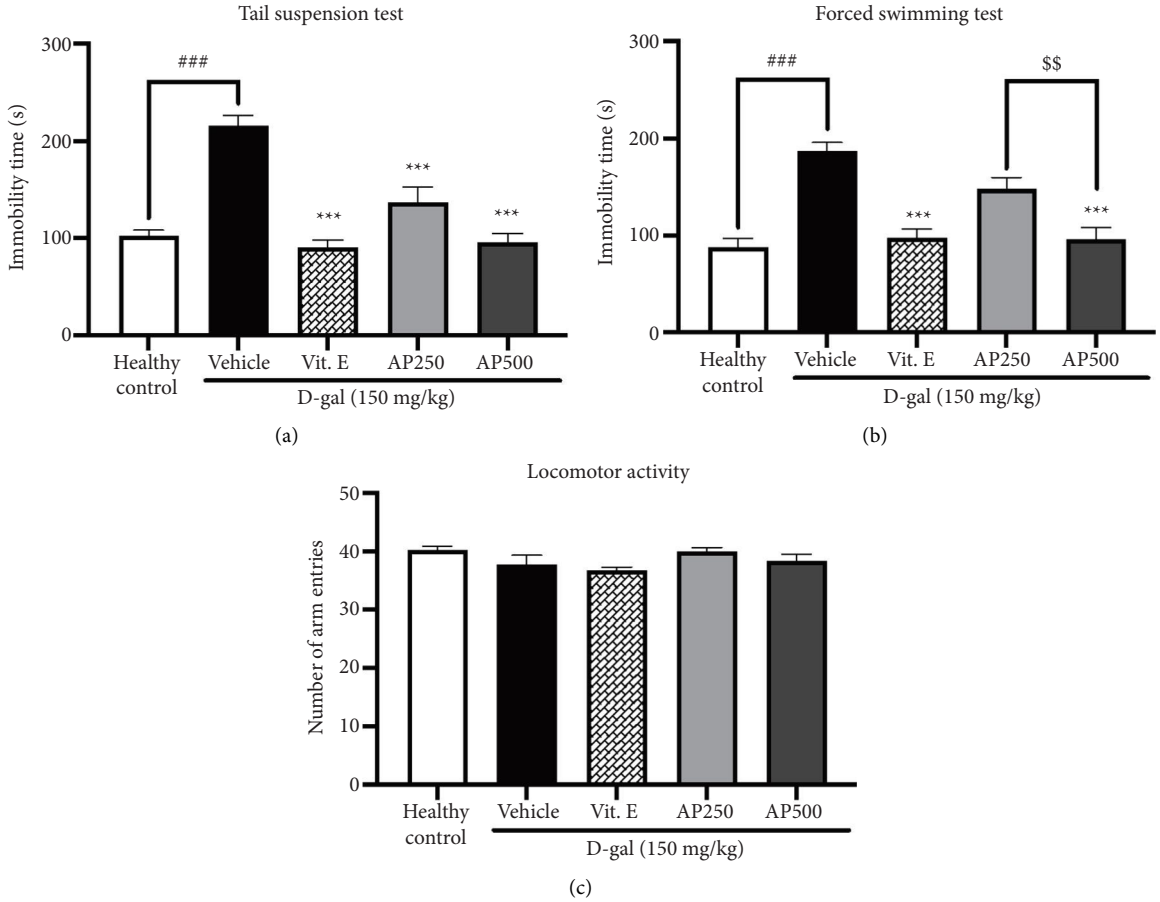


Figure 3: Immobility time from (a) TST and (b) FST exhibited behavioral despair in mice. (c) Locomotor activity was determined as the number of arm entries in the Y-maze test. Each data column represents the mean ± SEM ($n = 10$) and $^{###}p < 0.001$ vs. the healthy control group; $^{***}p < 0.001$ vs. the vehicle-treated group; and $^{\$\$}p < 0.01$ vs. the AP-treated group (post hoc Tukey test).

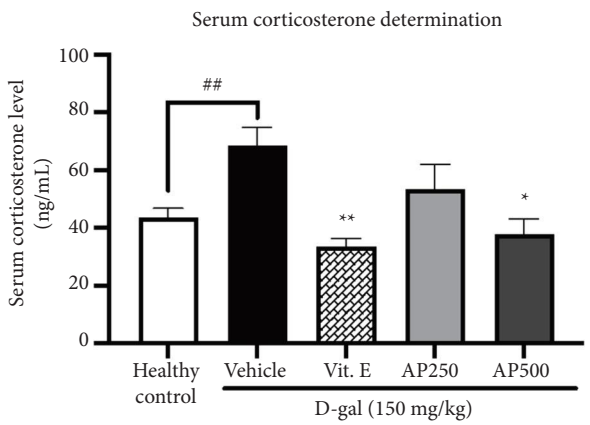


Figure 4: Stress exacerbation induced by D-gal was alleviated as a result of administering AP 500 mg/kg/day or vitamin E 100 mg/kg/day. Each data point represents the mean ± SEM ($n = 6$) $^{##}p < 0.01$ vs. the healthy control group; $^{*}p < 0.05$, and $^{**}p < 0.01$ vs. the vehicle-treated group (post hoc Tukey test).

Four metabolic pathways were found to demonstrate statistically significant changes with an impact value > 0.1 after these significantly detected metabolites were subjected

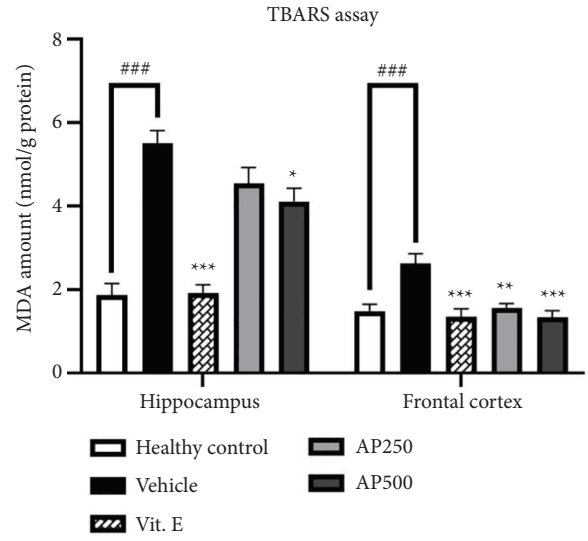


Figure 5: The MDA levels reflected oxidative degradation in the hippocampus and frontal cortex. Each data point represents the mean ± SEM ($n = 6$) $^{###}p < 0.001$ vs. the healthy control group; $^{*}p < 0.05$, $^{**}p < 0.01$, and $^{***}p < 0.001$ vs. the vehicle-treated group (post hoc Tukey test).

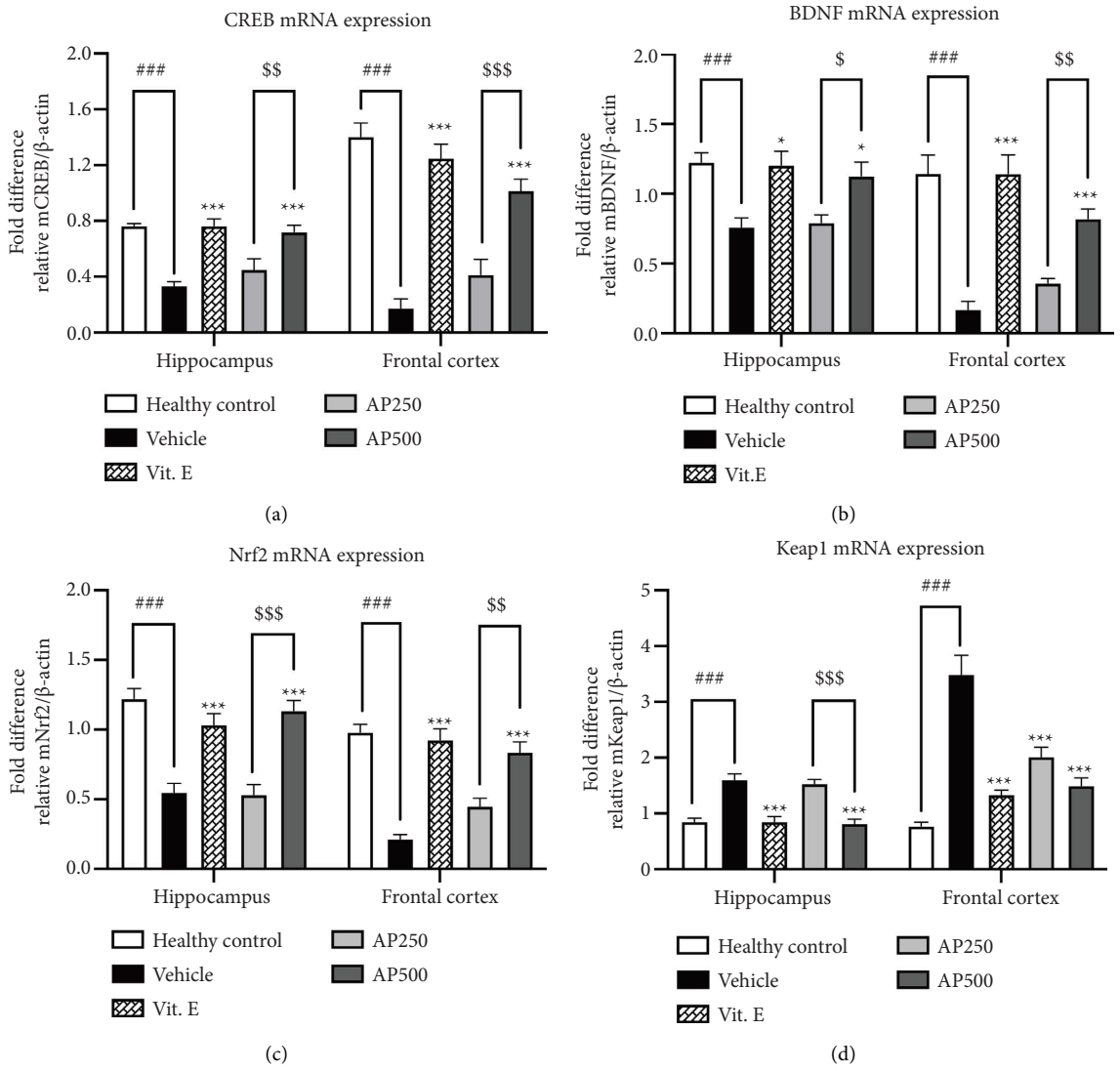


Figure 6: The gene expression of (a) CREB, (b) BDNF, (c) Nrf2, and (d) Keap1 was involved in the promotion of neurogenesis and the enhancement of the endogenous antioxidative response. Each column represents the mean ± SEM ($n = 6$) $^{###}p < 0.001$ vs. the healthy control group; $^{*}p < 0.05$, $^{***}p < 0.001$ vs. the vehicle-treated group; $^{\$\$}p < 0.01$, and $^{\$\$\$}p < 0.001$ vs. the AP-treated group (post hoc Tukey test).

to metabolic pathway analysis (Supporting Information, Table S3). The results are shown in a metabolic pathway analysis plot in Figure 10. The pathways included the production of phenylalanine, tyrosine, and tryptophan (aromatic amino acid biosynthesis) and metabolism of phenylalanine and tyrosine, as well as the tricarboxylic acid (TCA) cycle.

4. Discussion

AP has previously been shown to exert antidepressive effects in OVX mice, a model that mimics estrogen deprivation and simulates a perimenopausal or postmenopausal state. This estrogenic-like activity of AP has been associated with its modulatory effects on neuroinflammation and neuroplasticity that may alleviate depression in OVX mice [6]. In the present study, Chronic D-gal administration was used to induce depression in ICR mice by accelerating aging-associated neurodegeneration. D-gal triggers depression through several intricate processes, such as oxidative stress, neuroinflammation, and alteration of neurotransmitter networks [9, 19]. Consistent with previous findings, exacerbated depressive symptoms in aging mice were associated with higher levels of stress hormones, brought about by oxidative damage in the brain that alters the expression of genes regulating oxidative stress and neurotrophic factors.

Mechanistically, aging-induced depression is associated with the impairment of two key cellular pathways, i.e., the Nuclear Factor Erythroid 2–related factor (Nrf2) and cyclic adenosine monophosphate (cAMP) response element binding protein (CREB) and brain-derived neurotrophic factor (BDNF) (CREB–BDNF). The Nrf2 pathway plays a vital role in cellular antioxidant defense. Nrf2 translocation to the nucleus facilitates the upregulation of antioxidant response elements (AREs) that counteract oxidative stress. However, Nrf2 may be suppressed by Kelch-like ECH–

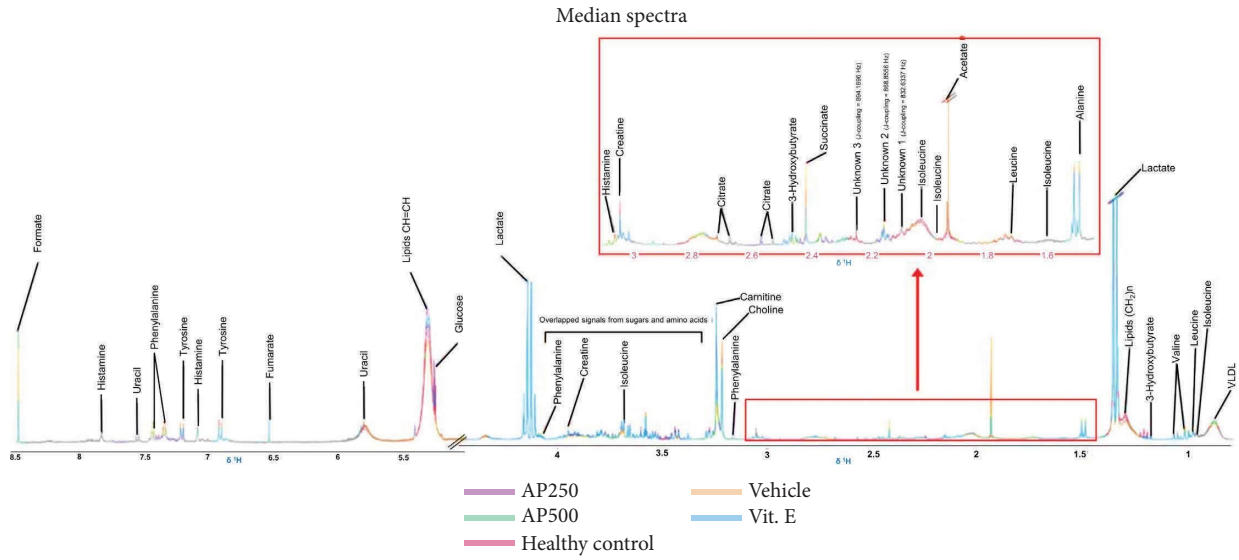


Figure 7: Median spectra of serum samples indicating detected metabolites.

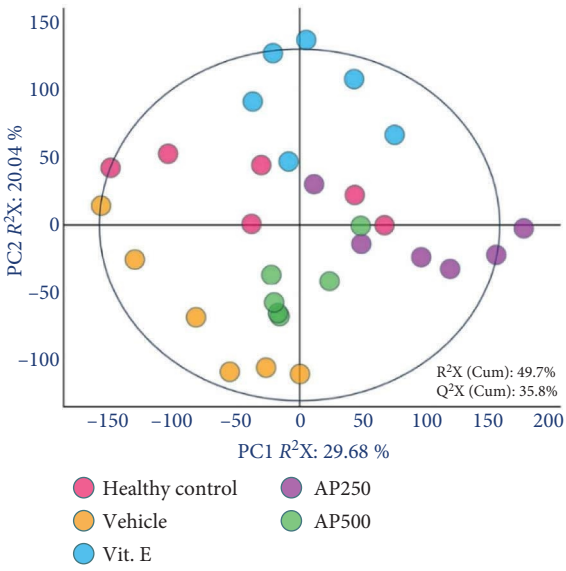


Figure 8: PCA score plot for overall metabolomic dataset of all experimental groups.

associated Protein 1 (Keap1) in the absence of cellular stress [20]. Two neurotrophic factors supporting neurogenesis and synaptic plasticity include CREB–BDNF [21]. Impairment in these pathways leads to increased oxidative damage and diminished neurogenesis, further contributing to depression. Our findings suggest that the AP extract may not only be associated with strengthening endogenous antioxidative defenses, but also be suggested to modulate neurogenesis. These effects align with the neuroprotective and mood-stabilizing properties and provide an additional perspective on the multifaceted mechanisms through which AP alleviates depressive symptoms (Figure 11).

As the chemical structures of isoflavone constituents provide antioxidative properties, they exert radical scavenging activities via both single-electron transfer and hydrogen atom transfer [22]. The capacity of AP extract to scavenge prominent oxidative radicals such as hydrogen peroxide and hydroxyl radical was demonstrated. After D-gal -induced mice were treated with AP extract, the internal defensive capacity was restored, as observed by the upregulation of AREs and protection against lipid oxidative damage in the brain. These findings suggest that the isoflavone constituents of AP exert antioxidant activities and provide critical preventive effects that mitigate oxidative damage to neurons, a key contributor to age-related depression. Additionally, AP extract facilitated neurogenesis by fostering an environment conducive to neuronal growth and repair due to the modulation of neurotrophic factors apart from telomere-stabilizing properties previously reported by Aon-im et al. [9]. Therefore, AP not only prevented cellular aging by promoting cellular resilience and protecting neuronal cells from senescence but also actively contributed to nervous tissue regeneration. The potential synergy between cellular longevity and regenerative capacity supports a comprehensive framework for enhancing brain health in aging populations [23]. AP also restored the HPA axis from inflammation-induced hyperactivation. The anti-inflammatory properties of AP, previously reported by Aon-im et al. [9], along with the antioxidant activities, normalized corticosterone levels. These beneficial effects prevented stress responsiveness, resulting in depression.

The capacity of AP extract in ameliorating depressive symptoms is attributed to its modulation of multiple metabolic pathways, which are integral to normalizing brain function and countering neurochemical imbalances associated with aging-induced depression. The biosynthetic pathway of aromatic amino acids (i.e., phenylalanine, tyrosine, and tryptophan) and phenylalanine and tyrosine metabolism involve the synthesis of key precursors for neurotransmitters (e.g., dopamine, serotonin, and norepinephrine) that play a substantial role in mood regulation. For example, phenylalanine is metabolized into tyrosine, which is further converted into dopamine. Disruptions in

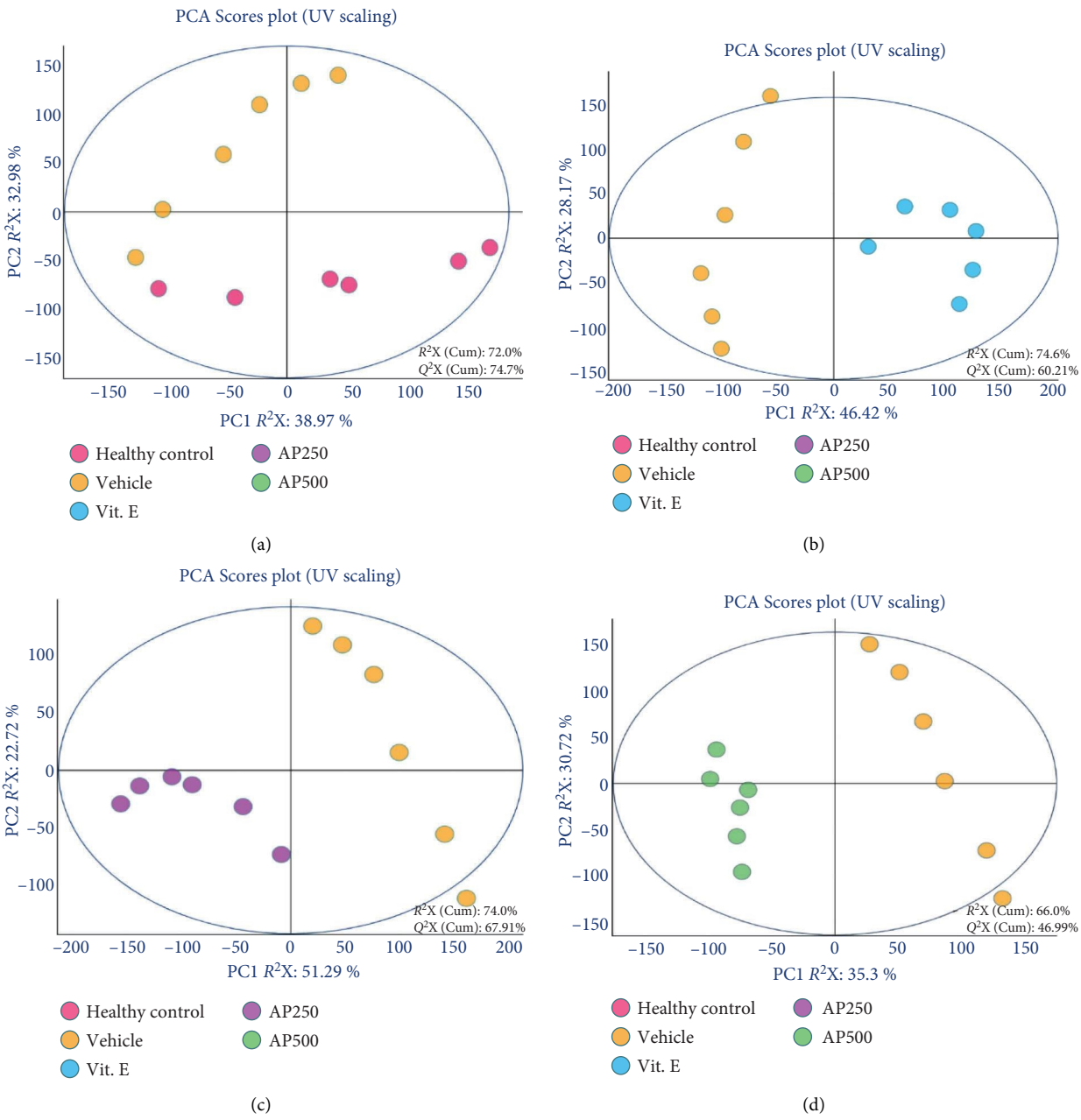


Figure 9: Continued.

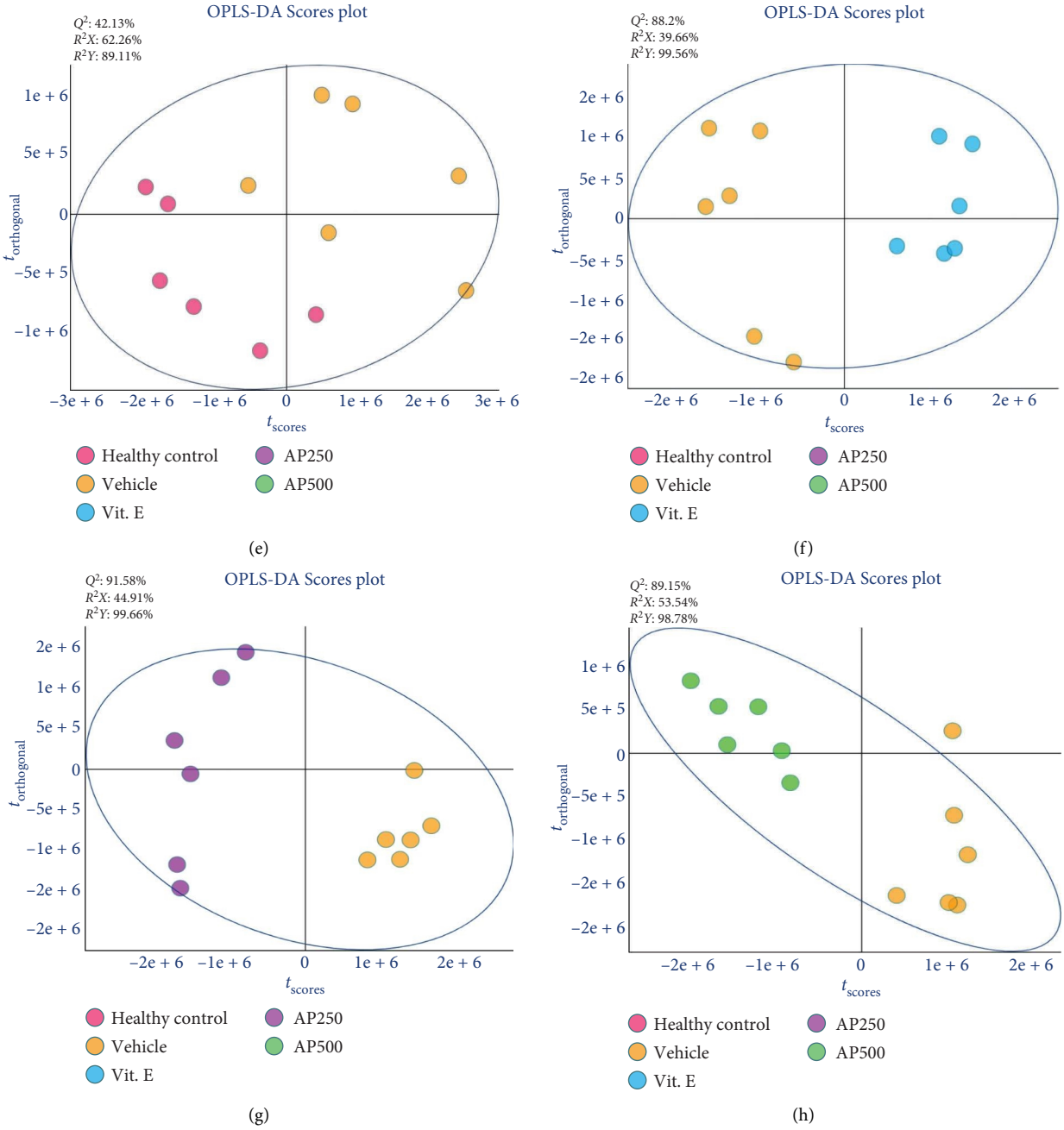


Figure 9: Pairwise comparison of each experimental groups. (a) Healthy control vs. vehicle; (b) vehicle vs. Vit. E; (c) vehicle vs. AP250; (d) vehicle vs. AP500, using PCA modeling. (e) healthy control vs. vehicle; (f) vehicle vs. Vit. E; (g) vehicle vs. AP250; (h) vehicle vs. AP500, using OPLS-DA study.

phenylalanine, tryptophan, or tyrosine production, as well as phenylalanine metabolism, may lead to depression symptoms and alterations of the functional brain network from insufficient neurotransmitter levels [24]. Furthermore, the citrate cycle (TCA cycle) plays a crucial role in aging and brain energy metabolism, as it is closely linked to mitochondrial function and serves as a central pathway for energy production. A decline in the activity and quality of mitochondrial function may further facilitate the development of age-related diseases. The TCA cycle also produces ROS as by-products of the electron transport chain [25]. Enhancing TCA cycle activity through dietary interventions, pharmacological agents, or metabolic precursors may offer therapeutic potential in mitigating age-related neurodegeneration and promoting longevity [26]. The current results show that D-gal vehicle–treated mice exhibited decreased Nrf2 and increased Keap1 mRNA expression in both the frontal cortex and hippocampus, all of which were restored by AP extract treatment. The Nrf2-Keap1 pathway plays an important role in protecting against oxidative stress and regulating antioxidant responses, which involves neuron damage [20]. Dysregulation of CREB activity impairs the

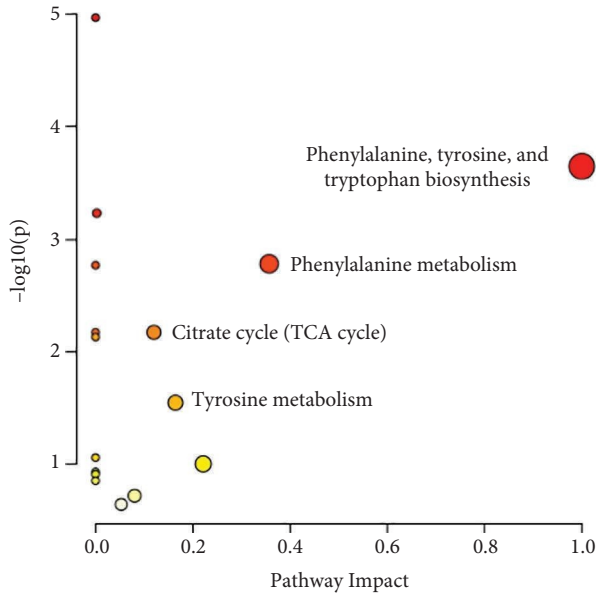


Figure 10: Metabolic pathway analysis plot.

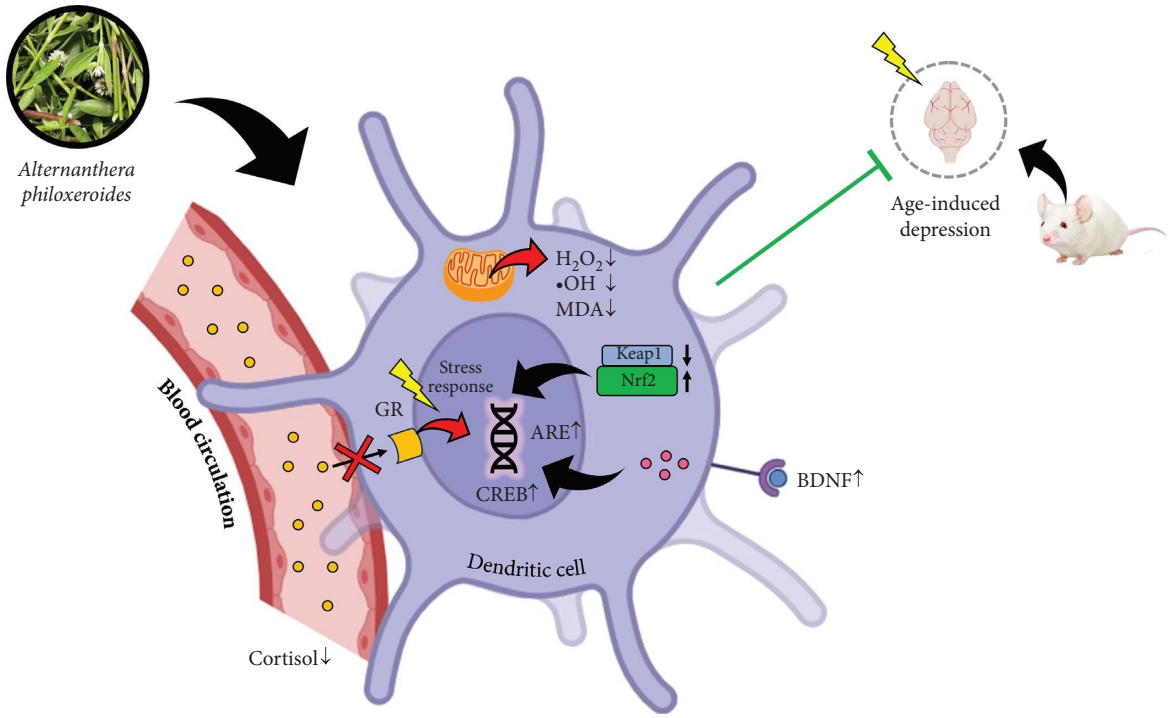


Figure 11: The possible mechanism of action of AP extract.

transcription of BDNF genes essential for neurogenesis and neuron plasticity, while reduced CREB activation leads to decreased BDNF expression, potentially contributing to the development of depression [6].

The behavioral assessments revealed that AP treatment of D-gal–treated mice led to a notable reduction in depressive-like behaviors, as evidenced by lower levels of hopelessness compared to the D-gal vehicle–treated group. The isoflavone constituents of AP were isolated, i.e., alternanthin, Alternanthin B, Torosaflavone E, Demethyltorosaflavone D, and Chrysoeriol 7-O-rhamnoside, were found to inhibit MAO inhibitory activity [6]. Furthermore, the ethanol extract of AP used in this study was analyzed, and kaempferol-O-glucoside, quercetin, alternanthin, Alternanthin B, Demethyltorosaflavone D, and Chrysoeriol 7-O-rhamnoside were identified as major constituents. Hence, these compounds are significantly associated with antidepressive potential against aging-induced depression. The greater efficacy observed with 500 mg/kg/day of AP extract compared to 250 mg/kg/day may reflect several interrelated factors. First, antidepressant-like effects of

phytochemicals often follow a dose–response relationship, where a minimal threshold must be exceeded to achieve robust engagement of neuroprotective and neurotrophic pathways. Second, despite the numerous health advantages of flavonoids being demonstrated via several in vitro studies, their poor bioavailability, which would affect the bioactivities in vivo, has raised concerns [27]. The higher dose may be necessitated to ensure sufficient systemic and brain exposure for coordinated behavioral and molecular improvements. Together, these considerations suggest that 500 mg/kg/day provided a more complete target engagement and functional outcome than the lower dose. Collectively, these findings position AP as a promising candidate for developing natural antidepressant therapies for age-related neurodegenerative conditions, offering a multifactorial approach to depression treatment that targets oxidative stress, neurogenesis, and essential metabolic pathways. However, this study has limitations. First, the animal model may not fully recapitulate human depression's multifactorial etiology involving psychosocial, genetic, and environmental factors. Second, D-gal–induced depression primarily models oxidative stress-related neurodegeneration and may not translate to other depression subtypes. Third, pharmacokinetic differences between mice and humans necessitate careful dose extrapolation for clinical application.

Future studies should include toxicity testing should be performed to identify potential adverse effects and evaluate the dose-response relationship, as well as pharmacokinetic studies to determine absorption, distribution, metabolism, and excretion of AP's active constituents. Additional preclinical models, including chronic stress or genetic depression paradigms, could further validate therapeutic potential. Ultimately, well-designed clinical trials are essential to confirm efficacy and safety in humans.

5. Conclusion

Long-term exposure to D-gal can mimic aging characteristics related to age-related diseases. In this study, neuronal damage was promoted by oxidative stress even though the capacities of defensive and regenerative systems were limited. Neurodegeneration subsequently occurred and initiated the progression of neurodegenerative diseases, especially depression. However, the AP treatment was able to restore neuronal deterioration. The notable enhancement in neuroprotection, counteraction against cellular damage, and promotion of neurogenesis were reported. This study highlights the antidepressive potential of AP against aging-induced depression. AP may be a promising herbal preparation for further development as an antidepressant for elderly patients. However, further research in models of other neurological ailments is necessary to explore novel treatment strategies for improving the quality of life in the elderly.

Nomenclature

AGEs	advanced glycation end products
ANOVA	one-way analysis of variance
AP	*Alternanthera philoxeroides*
AREs	antioxidant response elements
BCAAs	branched-chain amino acids
BDNF	brain-derived neurotrophic factor
cDNA	complementary DNA
CoA	coenzyme A
CREB	cAMP response element binding protein
D-gal	D-galactose
DPPH	2,2-diphenyl-1-picrylhydrazyl
FID	free induction decay
FRAP	ferric reducing antioxidant power
FST	forced swimming test
HPA	hypothalamic–pituitary–adrenal
IC_{50}	half-maximal inhibitory concentration
Keap1	Kelch-like ECH-associated protein 1
LA	locomotor activity
MAO	monoamine oxidase
MDA	malondialdehyde
Nrf2	Nuclear Factor Erythroid 2–related factor 2
OPLS-DA	orthogonal partial least squares discriminant analysis
OVX	ovariectomized
PCA	principal component analysis
ROS	reactive oxygen species
TBARS	thiobarbituric acid reactive substance
TST	tail suspension test.

Data Availability Statement

Data are available on request from the authors.

Ethics Statement

The authors state that animal use in this study was approved by the Institutional Animal Care and Use Committee of Khon Kaen University, Thailand (Record: IACUC-KKU-77/65; Reference: 660201.2.11/512(82)).

Conflicts of Interest

The authors declare no conflicts of interest.

Author Contributions

Charinya Khamphukdee: conceptualization, funding acquisition, methodology, validation, data curation, and writing–review and editing. Possatorn Aon-im: data curation, investigation, methodology, formal analysis, and writing–original draft. Orawan Monthakantirat, Yaowared Chulikhit, and Supawadee Daodee: resources, methodology, supervision, and validation. Chantana Boonyarat: resources, methodology, and validation. Anake Kijjoa: resources, investigation, and review and editing.

Funding

Financial support for this investigation was provided by the Research Grant for New Scholars (RGNS 64–041) and the Fundamental Fund of Khon Kaen University's 2023 program (Grant No. 4708091).

Acknowledgments

The authors sincerely acknowledge the Office of the Ministry of Higher Education, Sciences, and Innovation under the Reinventing University 2024 Visiting Professor Program. We would like to declare that generative Al (Claude-4.5) was used solely for assistance in checking and refining the English language in this manuscript, including minor translations. The authors entirely generated the content, ideas, and findings presented in the manuscript without Al assistance. After language editing, the authors reviewed and validated the final version. We would like to thank Editage (https://www.editage.com) for editing and reviewing this manuscript for English language.

Supporting Information

Additional supporting information can be found online in the Supporting Information section. *(Supporting Information)*

Supporting Figure S1: Phytochemical profiles analyzed by high-performance liquid chromatography (HPLC). Supporting Table S2: Detected metabolites with corresponding chemical shifts (δ, ppm), regression coefficients (β), VIP scores, and Bonferroni-adjusted p values contributing to the discrimination between vehicle and AP500 groups. Supporting Figure S2: Permutation test validating the robustness and reliability of the OPLS-DA model of group separation between vehicle and AP500. Supporting Table S3: The revealed pathways related to significantly elevated metabolites from the AP extract 500 mg/kg/day.

References

[1] A. Houldsworth, "Role of Oxidative Stress in Neurodegenerative Disorders: A Review of Reactive Oxygen Species and Prevention by Antioxidants," *Brain Commun* 6, no. 1 (2023): fcad356, https://doi.org/10.1093/braincomms/fcad356.

[2] E. Knezevic, K. Nenic, V. Milanovic, and N. N. Knezevic, "The Role of Cortisol in Chroni Stress, Neurodegenerative Diseases, and Psychological Disorders," *Cells* 12, no. 23 (2023): 2726, https://doi.org/10.3390/cells12232726.

[3] H. Tian, Z. Hu, J. Xu, and C. Wang, "The Molecular Pathophysiology of Depression and the New Therapeutics," *MedComm* 3, no. 3 (2022): e156, https://doi.org/10.1002/mco2.156.

[4] A. Rattanathongkom, J.-B. Lee, K. Hayashi, B. Sripanidkulchai, T. Kanchanapoom, and T. Hayashi, "Evaluation of Chikusetsusaponin IVa Isolated from *Alternanthera philoxeroides* for its Potency Against Viral Replication," *Planta Medica* 75, no. 8 (2009): 829–835, https://doi.org/10.1055/s-0029-1185436.

[5] S. S. Khandker, M. Alam, F. Uddin, et al., "Subchronic Toxicity Study of *Alternanthera philoxeroides* in Swiss Albino Mice Having Antioxidant and Anticoagulant Activities," *Journal of Toxicology* ed. R. Tanguay, 2022 (2022): 1–12, https://doi.org/10.1155/2022/8152820.

[6] C. Khamphukdee, O. Monthakantirat, Y. Chulikhit, et al., "Chemical Constituents and Antidepressant-Like Effects in Ovariectomized Mice of the Ethanol Extract of *Alternanthera philoxeroides*," *Molecules* 23, no. 9 (2018): 2202, https://doi.org/10.3390/molecules23092202.

[7] C. Bo-Htay, S. Palee, N. Apaijai, S. C. Chattipakorn, and N. Chattipakorn, "Effects of D-galactose-induced Ageing on the Heart and its Potential Interventions," *Journal of Cellular and Molecular Medicine* 22, no. 3 (2018): 1392–1410, https://doi.org/10.1111/jcmm.13472.

[8] N. Samad, F. Hafeez, and I. Imran, "D-galactose Induced Dysfunction in Mice Hippocampus and the Possible Antioxidant and Neuromodulatory Effects of Selenium," *Environmental Science & Pollution Research* 29, no. 4 (2022): 5718–5735, https://doi.org/10.1007/s11356-021-16048-x.

[9] P. Aon-im, O. Monthakantirat, S. Daodee, et al., "Evaluation of the Impact of *Alternanthera philoxeroides* (Mart) Griseb. Extract on Memory Impairment in D-Galactose-Induced Brain Aging in Mice Through Its Effects on Antioxidant Enzymes, Neuroinflammation, and Telomere Shortening," *Molecules* 29, no. 2 (2024): 503, https://doi.org/10.3390/molecules29020503.

[10] D. Mukhopadhyay, P. Dasgupta, D. Sinha Roy, et al., "A Sensitive in Vitro Spectrophotometric Hydrogen Peroxide Scavenging Assay Using 1,10-Phenanthroline," *Free Radicals and Antioxidants* 6, no. 1 (2016): 124–132, https://doi.org/10.5530/fra.2016.1.15.

[11] R. Roghini and K. Vijayalakshmi, "Free Radical Scavenging Activity of Ethanolic Extract of Citrus Paradisi and Naringin-An in Vitro Study," *International Journal of Pharmacognosy and Phytochemical Research* 10, no. 1 (2018): 11–16, https://doi.org/10.25258/phyto.v10i01.11925.

[12] A. Othman, A. Ismail, F. A. Hassan, B. N. M. Yusof, and A. Khatib, "Comparative Evaluation of Nutritional Compositions, Antioxidant Capacities, and Phenolic Compounds of Red and Green Sessile Joyweed (Alternanthera sessilis)," *Journal of Functional Foods* 21 (2016): 263–271, https://doi.org/10.1016/j.jff.2015.12.014.

[13] D. Skroza, I. G. Mekinić, S. Svilović, V. Šimat, and V. Katalinić, "Investigation of the Potential Synergistic Effect of Resveratrol with Other Phenolic Compounds: A Case of Binary Phenolic Mixtures," *Journal of Food Composition and Analysis* 38 (2015): 13–18, https://doi.org/10.1016/j.jfca.2014.06.013.

[14] S. Daodee, O. Monthakantirat, K. Ruengwinitwong, et al., "Effects of the Ethanol Extract of Dipterocarpus alatus Leaf on the Unpredictable Chronic Mild Stress-Induced Depression in ICR Mice and Its Possible Mechanism of Action," *Molecules* 24, no. 18 (2019): 3396, https://doi.org/10.3390/molecules24183396.

[15] J. Maneenet, S. Daodee, O. Monthakantirat, et al., "Kleeb Bua Daeng, a Thai Traditional Herbal Formula, Ameliorated Unpredictable Chronic Mild Stress-Induced Cognitive Impairment in ICR Mice," *Molecules* 24, no. 24 (2019): 4587, https://doi.org/10.3390/molecules24244587.

[16] C. Chalermwongkul, C. Khamphukdee, J. Maneenet, et al., "Antidepressant-Like Effect of Oroxylum indicum Seed Extract in Mice Model of Unpredictable Chronic Mild Stress," *Nutrients* 15, no. 22 (2023): 4742, https://doi.org/10.3390/nu15224742.

[17] W. N. Arifin, W. M. Zahiruddin, Department of Community Medicine, et al., "Sample Size Calculation in Animal Studies Using Resource Equation Approach," *Malaysian Journal of Medical Sciences* 24, no. 5 (2017): 101–105, https://doi.org/10.21315/mjms2017.24.5.11.

[18] P. Virtanen, R. Gommers, T. E. Oliphant, et al., "Scipy 1.0: Fundamental Algorithms for Scientific Computing in Python," *Nature Methods* 17, no. 3 (2020): 261–272, https://doi.org/10.1038/s41592-019-0686-2.

[19] Y. Zhang, Z. Pi, F. Song, and Z. Liu, "Ginsenosides Attenuate d-galactose- and AlCl3-induced Spatial Memory Impairment by Restoring the Dysfunction of the Neurotransmitter Systems in the Rat Model of Alzheimer's Disease," *Journal of Ethnopharmacology* 194 (2016): 188–195, https://doi.org/10.1016/j.jep.2016.09.007.

[20] D. Akin-Bali, T. Eroglu, S. Ilk, Y. Egin, and T. Kankilic, "Evaluation of the Role of Nrf2/Keap1 pathway-associated Novel Mutations and Gene Expression on Antioxidant Status in Patients with Deep Vein Thrombosis," *Experimental and Therapeutic Medicine* 20, no. 2 (2020): 868–881, https://doi.org/10.3892/etm.2020.8790.

[21] M. Miranda, J. F. Morici, M. B. Zanoni, and P. Bekinschtein, "Brain-Derived Neurotrophic Factor: A Key Molecule for Memory in the Healthy and the Pathological Brain," *Frontiers in Cellular Neuroscience* 13 (2019): 363, https://doi.org/10.3389/fncel.2019.00363.

[22] N. Mohammadi, A. Dos Santos Lima, L. Azevedo, and D. Granato, "Bridging the Gap in Antioxidant Activity of Flavonoids: Correlating the Oxidation of Human Plasma with Chemical and Cellular Assays," *Current Research in Food Science* 8 (2024): 100714, https://doi.org/10.1016/j.crfs.2024.100714.

[23] A. B. Palmos, R. R. R. Duarte, D. M. Smeeth, et al., "Telomere Length and Human Hippocampal Neurogenesis," *Neuropsychopharmacology* 45, no. 13 (2020): 2239–2247, https://doi.org/10.1038/s41386-020-00863-w.

[24] S. Zhao, S. Khoo, S.-C. Ng, and A. Chi, "Brain Functional Network and Amino Acid Metabolism Association in Females with Subclinical Depression," *International Journal of Environmental Research and Public Health* 19, no. 6 (2022): 3321, https://doi.org/10.3390/ijerph19063321.

[25] N. Sun, R. J. Youle, and T. Finkel, "The Mitochondrial Basis of Aging," *Molecular Cell* 61, no. 5 (2016): 654–666, https://doi.org/10.1016/j.molcel.2016.01.028.

[26] H. Liu, S. Wang, J. Wang, et al., "Energy Metabolism in Health and Diseases," *Signal Transduction and Targeted Therapy* 10, no. 1 (2025): 69, https://doi.org/10.1038/s41392-025-02141-x.

[27] S. Thilakarathna and H. Rupasinghe, "Flavonoid Bioavailability and Attempts for Bioavailability Enhancement," *Nutrients* 5, no. 9 (2013): 3367–3387, https://doi.org/10.3390/nu5093367.